European Journal of Agronomy 111 (2019) 125937

Contents lists available at ScienceDirect

European Journal of Agronomy

journal homepage: www.elsevier.com/locate/eja

Identifying the most promising agronomic adaptation strategies for the tomato growing systems in Southern Italy *via* simulation modeling

Marcella Michela Giuliani[a], Giuseppe Gatta[a], Giovanni Cappelli[b], Anna Gagliardi[a], Marcello Donatelli[b], Davide Fanchini[b], Dario De Nart[b], Gabriele Mongiano[c], Simone Bregaglio[b,*]

[a] Department of Agricultural Food and Environmental Science, University of Foggia, via Napoli 25, 71122, Foggia, Italy
[b] CREA – Council for Agricultural Research and Economics, Research Centre for Agriculture and Environment, via di Corticella 133, 40128, Bologna, Italy
[c] CREA – Council for Agricultural Research and Economics, Research Centre for Plant Protection and Certification, SS 11 km 2,500, 13100, Vercelli, Italy

ARTICLE INFO

Keywords:
Climate change
Crop simulation model
Deficit irrigation
Fruit quality
Processing tomato
Water stress

ABSTRACT

The main cultivation area of the Italian processing tomato is the Southern Capitanata plain. Here, the hardest agronomic challenge is the optimization of the irrigation water use, which is often inefficiently performed by farmers, who tend to over-irrigate. This could become unsustainable in the next years, given the negative impacts of climatic changes on groundwater availability and heat stress intensification. The aim of the study was to identify the most promising agronomic strategies to optimize tomato yield and water use in Capitanata, through a modeling study relying on an extensive dataset for model calibration and evaluation (22 data sets in 2005–2018). The TOMGRO simulation model was adapted to open-field growing conditions and was coupled with a soil model to reproduce the impact of water stress on yield and fruit quality. The new model, TomGro_field, was applied on the tomato cultivation area in Capitanata at 5 × 5 km spatial resolution using an ensemble of future climatic scenarios, resulting from the combination of four General Circulation Models, two extreme Representative Concentration Pathways and five 10-years time frames (2030–2070). Our results showed an overall negative impact of climate change on tomato yields (average decrease = 5–10%), which could be reversed by i) the implementation of deficit irrigation strategies based on the restitution of 60–70% of the crop evapotranspiration, ii) the adoption of varieties with longer cycle and iii) the anticipation of 1–2 weeks in transplanting dates. The corresponding irrigation amounts applied are around 360 mm, thus reinforcing that a rational water management could be realized. Our study provides agronomic indications to tomato growers and lays the basis for a bio-economic analysis to support policy makers in charge of promoting the sustainability of the tomato growing systems.

1. Introduction

The global production of fresh and processing tomatoes increased by 300% during the last four decades (Costa and Heuvelink, 2007), reaching around 160 million tons in 2017 (Pathak and Stoddard, 2018). Italy, alongside China, India, Turkey and US, ranks among the top world tomato producers, and is the first producing country in Europe. The Italian tomato production accounts for nearly 6 million tons and is mostly concentrated in the Capitanata plain (Southern Italy), which alone has contributed to 33% of the total national amount in 2018 (ISTAT, 2018). In the last decade, the tomato production in Capitanata is facing many criticalities including workers exploitation and social unrests (Scotto, 2016), economic issues for tomato producers due to legislation changes (Giannoccaro et al., 2011) and environmental problems connected to the effects of the ongoing climatic changes (Ventrella et al., 2012), which are expected to be even larger in the upcoming years (Darand and Mansouri Daneshvar, 2015).

Tomato growing systems are highly intensive in this area, with a massive application of irrigation water (400–600 mm) and chemical inputs for fertilization and crop protection, with fresh fruits yields ranging between 80 and 160 t ha^{-1} (Rinaldi et al., 2011). The growing season spans between May and August and is characterized by scarce precipitations (average of 180 mm in 1981–2010) and temperatures often exceeding 40 °C, thus exposing the tomato plant to frequent heat and water stress during key phenological phases (Giuliani et al., 2019). Recent studies evidenced that the future climatic scenarios in semi-arid Mediterranean areas will be even more critical for crops, given the increase in the frequency and intensity of heat waves and the significant

* Corresponding author.
E-mail address: simoneugomaria.bregaglio@crea.gov.it (S. Bregaglio).

https://doi.org/10.1016/j.eja.2019.125937
Received 8 June 2019; Received in revised form 14 August 2019; Accepted 27 August 2019
1161-0301/ © 2019 The Authors. Published by Elsevier B.V. This is an open access article under the CC BY-NC-ND license (http://creativecommons.org/licenses/BY-NC-ND/4.0/).

rainfall decrease in summer (IPCC, 2007; Giorgi and Lionello, 2008; Vitale et al., 2010; Rubino et al., 2012). The large demand for irrigation water as well as the expected restriction of groundwater availability will force tomato growers to better rationalize the water use to sustain tomato yields and quality (Costa et al., 2007; Giuliani et al., 2017).

The common irrigation scheduling in current tomato growing systems comprises of fixed intervals between irrigation supplies without considering the actual crop water demand (Rinaldi et al., 2011), leading to over-irrigation and poor water use efficiency (Giuliani et al., 2016). The adoption of deficit irrigation (DI), which aims at optimizing the crop water productivity by limiting the water supply to a fraction of plant evapotranspiration (Zhang and Oweis, 1999; Geerts and Raes, 2009) could bring environmental and economic benefits. DI regimes indeed deliberately allow tomato crop sustaining some degree of water deficit, thus accepting small yield loss with an increase of fruits quality (Nuruddin et al., 2003) and a significant reduction in irrigation water use (Cantore et al., 2016).

The use of crop modeling to identify effective farmer strategies to counteract adverse future climatic conditions has become a standard in climate change impact assessments (Challinor et al., 2013; Asseng et al., 2015). This research area requires the integration of local-based knowledge into a modeling framework which proved to be capable to reproduce the real cropping systems, and the effects of alternative agricultural management strategies (Beveridge et al., 2018). In the last years, many research studies have tested and promoted DI strategies on tomato in open field conditions (Costa et al., 2007; Cantore et al., 2016; Giuliani et al., 2017), and have simulated the future trends of tomato production and water use under climate change scenarios (Ventrella et al., 2017).

In this study we calibrated and evaluated a new tomato simulation model using an extensive dataset of experiments carried out in open field conditions. We applied it in current and future climatic scenarios in order to evaluate for the first time the performances of tomato systems, testing the factorial combination of site-specific farming strategies. Thus, the aim of the present study is the identification of ready-to-use agronomic indications leading to the best trade-off in tomato yield, quality and water use, considering the DI strategy, the cycle length and the transplanting date.

2. Material and methods

2.1. Experimental trials for model calibration and evaluation

The field trials used for model calibration were carried out in 2017 and 2018 in Capitanata (41°46′N, 15°54′E, 74 m above the sea level). Processing tomato plants (*Solanum lycopersicum* L.) of *cv.* Ulisse F1 (S&G Syngenta Seeds S.p.A., Switzerland), characterized by elongated fruits, were hand-planted on May 3 (2017) and on April 27 (2018) in coupled rows spaced at 1.8 m, with plant density of 2.8 plants m^{-2} (0.50 m between rows, 0.40 m on the row). Four DI regimes were applied: DI_{100}, full irrigation, restoring 100% of the crop maximum evapotranspiration (ET_c); ii) DI_{75}, restoring 75% of ET_c; $DI_{75/50}$, restoring 75% of ET_c from transplanting to fruits breaking colours of the first truss, and 50% of ET_c from fruits breaking colours of the first truss to harvest; DI_0, irrigation only at transplanting and during fertigation. The cloud-based decision support system Bluleaf™ (Sysman Progetti e Servizi Srl, Rome, Italy), was used to estimate the amount of water supply of each irrigation event. This system is based on the data collected by wireless sensors (AgriSense™, Netsens, Florence, Italy) for real-time acquisition of weather and soil moisture data at 0.3 m and 0.6 m depth, which are used to compute daily ET_c. Daily reference evapotranspiration (ET_o) was calculated using the Penman-Monteith equation (Allen et al., 1989), and the crop coefficient (K_c) values were derived in an environment similar to our experimental site (Tarantino and Onofri, 1991). ET_c was estimated as $ET_o \times K_c$, following the FAO two-steps procedure (Allen et al., 1989). A drip irrigation system was used, composed by a single plastic pipe arranged in the middle of each paired row, with flow rate of 2 l h^{-1} and drippers spaced every 0.4 m. The amount of water supplied in each irrigation event was measured by flow meters placed on the main irrigation lines of the experimental fields (Table 1).

Table 1
Irrigation volumes, precipitation and total water received by tomato plants over the two growing seasons. DI_x = deficit irrigation restoring the *x* percentage of crop evapotranspiration. Please see main text for full explanation.

Year	Irrigation regime	Irrigation volume	Precipitation	Total water
		mm	mm	mm
2017	DI_{100}	358	268	626
	DI_{75}	276		544
	$DI_{75/50}$	240		508
	DI_0	45		313
2018	DI_{100}	310	212	522
	DI_{75}	238		450
	$DI_{75/50}$	199		411
	DI_0	35		247

The trials were arranged in a randomized block experimental design with four replicates, with each plot covering 30 m^2. The phenological stages of post-transplanting (S0), vegetative growth (S1), beginning of flowering (S2), fruit setting (S3) and fruit ripening (S4) have been recorded. In each growing season, nine destructive measurements of aerial plant organs biomass and leaf area index (LAI) were carried out on three plants per plot. At each sampling, the tomato plants were divided into leaves, stems and, when present, fruits. LAI was calculated as the ratio of total leaf area (m^2) per unit of ground area (m^2) using a leaf area meter (LI-3000, with conveyor belt assembly, LI-3050; Li-Cor, inc., Lincoln, NE, USA). Aerial plant biomass was expressed as plant dry mass obtained by oven-drying all the plant material at 70 °C until constant weight. The crop was hand-harvested when the rate of ripe fruits reached approximately 95%, on August 2 in 2017 and on July 30 in 2018. The fresh fruits yield was measured on six plants per plot, and the total soluble solids content (Degrees Brix, DB, °Brix) was assessed on 10 fruits $plot^{-1}$. DB was chosen as the main indicator of tomato quality, as it is highly correlated with the sweetness and maturity degree (Cahn et al., 2001), and directly affects fruit acceptability to buyers and consumers (*i.e.*, the higher the DB, the better the fruit quality). The fertilization practices and the pest and weed control replicated farmers' management practices typical of the area, aiming at growing the crop without any abiotic and biotic stress. Daily values of rainfall (mm), maximum and minimum air temperature (°C), relative air humidity (%) and average wind speed (m s^{-1}) were recorded by a weather station placed close to the experimental fields (Appendix A). An independent model evaluation was performed using reference data collected on comparable experimental field trials (2005–2016) performed with the tomato cv. Ulisse in Capitanata. These experiments were arranged to test the efficacy of DI regimes, with the measurement of fruit yield (t ha^{-1}) and DB at harvest (Table 2).

2.2. Adaptation of the TOMGRO greenhouse model to open field conditions

The object-oriented version of the process-based greenhouse tomato model TOMGRO (Jones, 1991) developed by Louski et al. (2013) was adapted to reproduce open field conditions to give a new tomato simulation model (TomGro_field). TOMGRO simulates the main processes associated with tomato growth and development as driven by air temperature, solar radiation and CO_2 concentration, providing a dynamic and deterministic simulation of the number and dry matter of stems, leaves and fruits. Seven main state variables are organized in vectors, whose size depends on the number of classes of physiological age, which was set to 10 in this study; the state variables are the numbers and dry weight of leaves, stems and fruits, and the leaves area.

Table 2
Experimental field trials carried out in 2005–2016 used for independent model evaluation, with deficit irrigation regime, volume, total solids soluble content (DB) and fruit yield.

Year	Deficit Irrigation	Irrigation volume	DB	Yield
		mm	° Brix	t ha^{-1}
2005	DI_{100}	503	5.0	84.54
	DI_{75}	382	5.2	85.84
	$DI_{75/100/75}$	440	5.3	91.34
	$DI_{50/75/50}$	331	5.0	79.92
	DI_{50}	272	5.8	70.44
2006	DI_{100}	477	4.7	97.15
	DI_{75}	365	4.9	78.26
	$DI_{75/100/75}$	420	5.0	73.46
	$DI_{50/75/50}$	311	5.4	83.97
	DI_{50}	250	4.8	67.15
2012	DI_{100}	565	5.1	94.97
	DI_{75}	375	5.1	60.88
2013	DI_{100}	516	5.1	97.44
	DI_{75}	391	6.3	66.65
	DI_{50}	208	6.3	51.27
	DI_0	40	7.7	28.24
2015	DI_{100}	459	5.3	134.14
	DI_{75}	360	5.7	105.52
2016	DI_{100}	396	4.7	125.74
	DI_{75}	304	5.4	111.58

The increase in the number of plant organs depends on the physiological development from one age class to the next and is driven by hourly temperature and CO_2 levels. The model simulates positive carbon fixation when the production rate of assimilates (source strength) overcomes the consumption rate (sink strength). The carbon sink strength of the tomato plant is computed summing the sink strengths of leaves, stems and fruits, which are based on their potential increase in dry weight (Jones, 1991). The photosynthetic process is simulated as net carbon assimilation, with hourly gross photosynthetic rate computed according to Acock et al. (1978), reduced by maintenance respiration losses (based on parameter Q10 and plant organs requirements) and growth respiration costs (fixed coefficient). The relative sink/source ratio also regulates the partitioning of dry matter into the different plant organs, with actual growth rates of leaves, stems and fruits obtained from their potential carbon demand. The full algorithmic description of TOMGRO is provided in the seminal paper, whereas the schematic description of the processes implemented in TomGro_field is presented in Fig. 1, which emphasise the modifications with respect to the original model. TomGro_field was implemented in the BioMA framework (Donatelli et al., 2014) as an independent software component and is available from the authors upon reasonable request.

The main modifications in TomGro_field addressed i) the reproduction of tomato phenological phases in open field growing conditions, *i.e.*, post-transplanting (S0), vegetative growth (S1), beginning of flowering (S2), fruit setting (S3) and fruit ripening (S4), using thermal time accumulation according to the review by Boote et al. (2012); ii) the simulation of leaves senescence, and the coupling of the plant model with a tipping-bucket model reproducing the dynamic of soil water availability and its impact on tomato growth, which were borrowed by CropSyst (Stockle et al., 1999); iii) the replacement of the table coefficients correlating state variables and parameter values with new functions driven by few parameters (Appendix B), following the approach developed by Stella et al. (2014); iv) the simulation of DB as a function of soil water availability and crop transpiration, with an impact on the qualitative aspects of tomato production (Cahn et al., 2001). DB (°Brix, Eq. (1)) has been simulated depending on the cumulated actual transpiration (AT_i, mm) in S3, modulated by the susceptibility to water stress (*fi*, unitless, cultivar-specific) and by parameters related to fruit development, growth and quality.

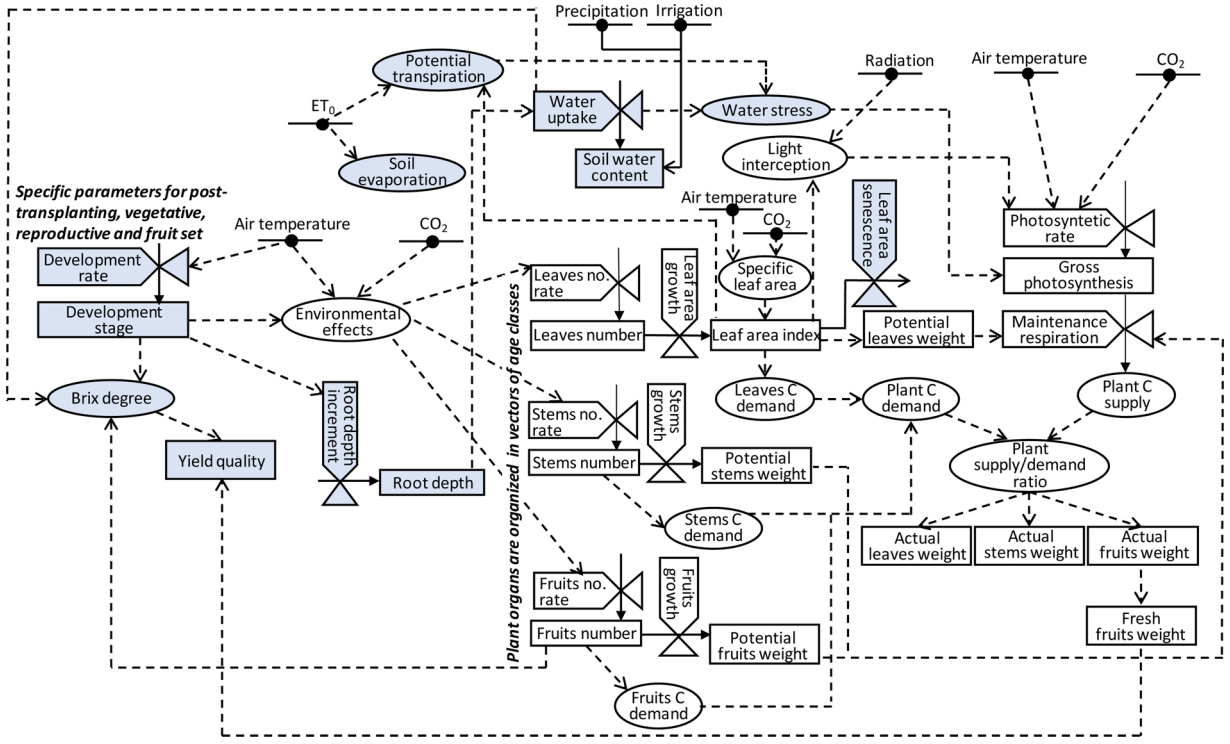

Fig. 1. Relational diagram of the TomGro_field model: air temperature, potential evapotranspiration (ET_0), precipitation, irrigation, radiation and CO_2 are driving variables. Rectangles denote system state variables, valve symbols denote rate variables and ovals denote intermediate or auxiliary variables. Solid lines denote flows of matter while broken lines are flows of information. The light blue color indicates the modifications to the original model. (For interpretation of the references to colour in this figure legend, the reader is referred to the web version of this article).

$$DB = -\frac{FN_{node}}{2} \cdot LN\left(\sum_{i=fruitsetIni}^{i=fruitsetEnd} f_i \cdot (AT_i)\right) + \frac{TD_{fruitset}}{SD_{fruitset}} \cdot DB_{\max} \quad (1)$$

where DB_{max} (°Brix) is the maximum DB, $SD_{fruitset}$ (days) is the number of days at which water stress sensitivity is halved; FN_{node} (unitless) and $TD_{fruitset}$ (thermal days) are the initial fruit number per node and the duration of fruit set phase, respectively. The daily values of *fi* (Eq. (2)) were derived by a logistic function driven by the number of days after fruit setting (DAF_i), and progressively decrease from 1 (maximum sensitivity) to 0 (no effect) as the fruit setting progresses.

$$f_i = \frac{1}{1 + \exp(SD_{fruitset} - DAF_i)} \quad (2)$$

2.3. Simulation experiment design

2.3.1. Model calibration and evaluation

TomGro_field was calibrated using the data collected in 2017 and 2018 experiments, before its independent evaluation using the historical field trials. The thermal time corresponding to the length of phenological phases were firstly calibrated according to field observations, following the standard methodology in crop modeling (Seidel et al., 2018; Leolini et al., 2018). Then, the parameters related to growth processes were adjusted: 11 parameters were measured in the field trials, 63 were fixed according to literature and 8 parameters were calibrated using the multi-start downhill simplex algorithm (Nelder and Mead, 1965; Acutis and Confalonieri, 2006). This automatic optimization method creates a simplex, which is a geometrical figure with N + 1 vertexes, with N as the number of parameters under evaluation. After each model run, the objective function is evaluated, and the model error is progressively minimized until the difference between consecutive runs drops below a tolerance range. The average relative root mean square error (RRMSE, minimum and optimum = 0%; maximum = + ∞, Jørgensen et al., 1986) in reproducing the dynamics of LAI, fresh fruits weight and dry weight of the plant organs was chosen as the objective function. We used 10 simplexes at each optimization run and 1000 iterations, with 0.001 as tolerance range. The DB model was calibrated on the whole experimental dataset using the Excel evolutionary solver and the modeling efficiency (EF, minimum = − ∞, maximum and optimum = 1, Nash and Sutcliffe, 1970) as objective function, and then evaluated *via* leave-one-out cross validation (LOOCV) according to Cappelli et al. (2018). The model performances in calibration and evaluation were quantified with standard metrics in crop modeling studies, *i.e.*, EF, RRMSE and mean absolute error (MAE, minimum and optimum = 0, maximum = + ∞, Schaeffer, 1980). Table C.1 (Appendix C) reports the values of the parameters, the literature sources and the ranges used for phenology, growth and fruit quality calibration. The model capability in reproducing the current tomato production levels in the area was further evaluated through spatially distributed simulations on the whole Capitanata plain (Appendix D, Fig. D.1), using a 5 × 5 km resolution in the period 1981–2010 (152 grid cells, Fig. 2).

2.3.2. Generation of baseline and future weather scenarios

Current climatic conditions in Capitanata (baseline scenario) were derived from daily weather series of temperature and rainfall in the period 1981–2010, which were available at 10 × 10 km spatial resolution (Appendix E, Fig. E.1). The available variables were the maximum and minimum air temperature (° C), precipitation (mm d^{-1}), global solar radiation (MJ m^{-2} d^{-1}), average wind speed (m s^{-1}) and evapotranspiration (mm d^{-1}). Hourly values of weather variables needed as input by TomGro_field were generated using the CLIMA components (Donatelli et al., 2005). The water content at saturation, the field capacity and the wilting point, were derived at 5 × 5 km resolution from soil texture and organic matter data (L'Abate et al., 2019) *via* pedotransfer functions (Saxton et al., 1986). Cartographic information related to orography and elevation in the region (http://www.sit.puglia.it/) were used to select the tomato harvested areas in Capitanata, setting 200 m a.s.l. as the upper-limit threshold. The soil and weather data were assigned to each grid cell using the geographic coordinates of centroids (Fig. 2) with QGIS software (v. 3.6.3. https://qgis.org/it/site/).

We used the CLIMAK weather generator (Danuso, 2002) to reproduce 30-years (1981–2010) of synthetic baseline weather series (Appendix E, Fig. E.1), and to generate future climatic scenarios (AR5, IPCC, 2013; Appendix E, Fig. E.2 and E3). The future scenarios corresponded to plausible impacts of the changes in atmospheric composition (IPCC, 2013) and referred to four General Circulation Models (GCMs) realizations of two CO_2 Representative Concentration Pathways in five 10-years time frames, centered on 2030–2070. The GCMs were selected according to Bregaglio et al. (2017) among the ones included in the Coupled Model Intercomparison Project (CMIP5, http://cmip-pcmdi.llnl.gov/cmip5/): the Norwegian Earth System Model (NOResm, Tjiputra et al., 2013), the Model for Interdisciplinary Research on Climate (MIROC-ESM, Watanabe et al., 2011), the Hadley Centre Global Environmental Model version 2 (HadGEM2-ES, Collins et al., 2011), and the GCM developed by the Goddard Institute for Space Studies (GISS-ES, Schmidt et al., 2006). The two extremes RCPs proposed by IPCC were used, 2.6 W m^{-2} and 8.5 W m^{-2}, to account for the maximum variability in radiative increase and CO_2 concentration (420 versus 936 cm^3 m^{-3} in 2100). The workflow to generate the future weather scenarios started with the computation of the monthly average anomalies (difference between the future and the present value of the variables; Déqué et al., 2007) of temperature and precipitation for each time frame corresponding to GCM × RCP combinations (Program for Climate Model Diagnosis and Intercomparison data portal (https://pcmdi.llnl.gov/search/cmip5/). These data were used as input to CLIMAK, which generated 20-years series for each of the 152 grid cells in Capitanata, considering the combination of 5 time frames (2030–2070), 4 GCM (NOResm, MIROC-ESM, HadGEM2-ES, GISS-ES) and 2 RCP (2.6, 8.5) leading to a total of 3040 climatic series.

2.3.3. Climate change impact assessment with adaptation

Spatially distributed simulations were performed in Capitanata using the baseline and future climatic data as input to TomGro_field. The annual simulated value of fresh fruit yield and DB were analysed, as well as their combination in a synthetic yield quality indicator of tomato production (Yield Quality, YQ, t ha^{-1}), based on local regulations (Framework agreement between producers organizations and processing industry, 2014, http://www.asipo.it/pdf/Allegato_Parametri_Qualitativi_2014.pdf, Eq. (3)).

$$YQ = \begin{cases} Y_{sim} \cdot 0.825 & if\ DB_{sim} \leq 4.3 \\ Y_{sim} \cdot (0.25 \cdot DB_{sim} - 0.25) & if\ 4.3 < DB_{sim} \leq 5.7 \\ Y_{sim} \cdot 1.175 & else \end{cases} \quad (3)$$

where Y_{sim} (t ha^{-1}) and DB_{sim} (°Brix) represent the yield and DB simulated at harvest. Water productivity (WP) was then computed considering the ratio between the total water applied to the crop (irrigation and precipitation) and the YQ indicator (Molden, 2003; Geerts and Raes, 2009). Four farmer adaptation strategies to climate change were selected according to place-based knowledge, aiming at their feasible implementation by tomato growers in Capitanata (Table 3). The strategies were: alternative DI regimes, the interval between two water supplies, the cultivation of tomato varieties with different cycle length and the shift in the transplanting dates.

Eleven DI strategies were tested, corresponding to a 10% increase of ET_c from rainfed (DI_0) to full irrigation (DI_{100}). The irrigation interval was set to 6 days in baseline conditions according to literature and experimental data, and ± 3 days were tested in future simulations. The duration of the growing cycle of the cv. Ulisse was varied by ± 10%

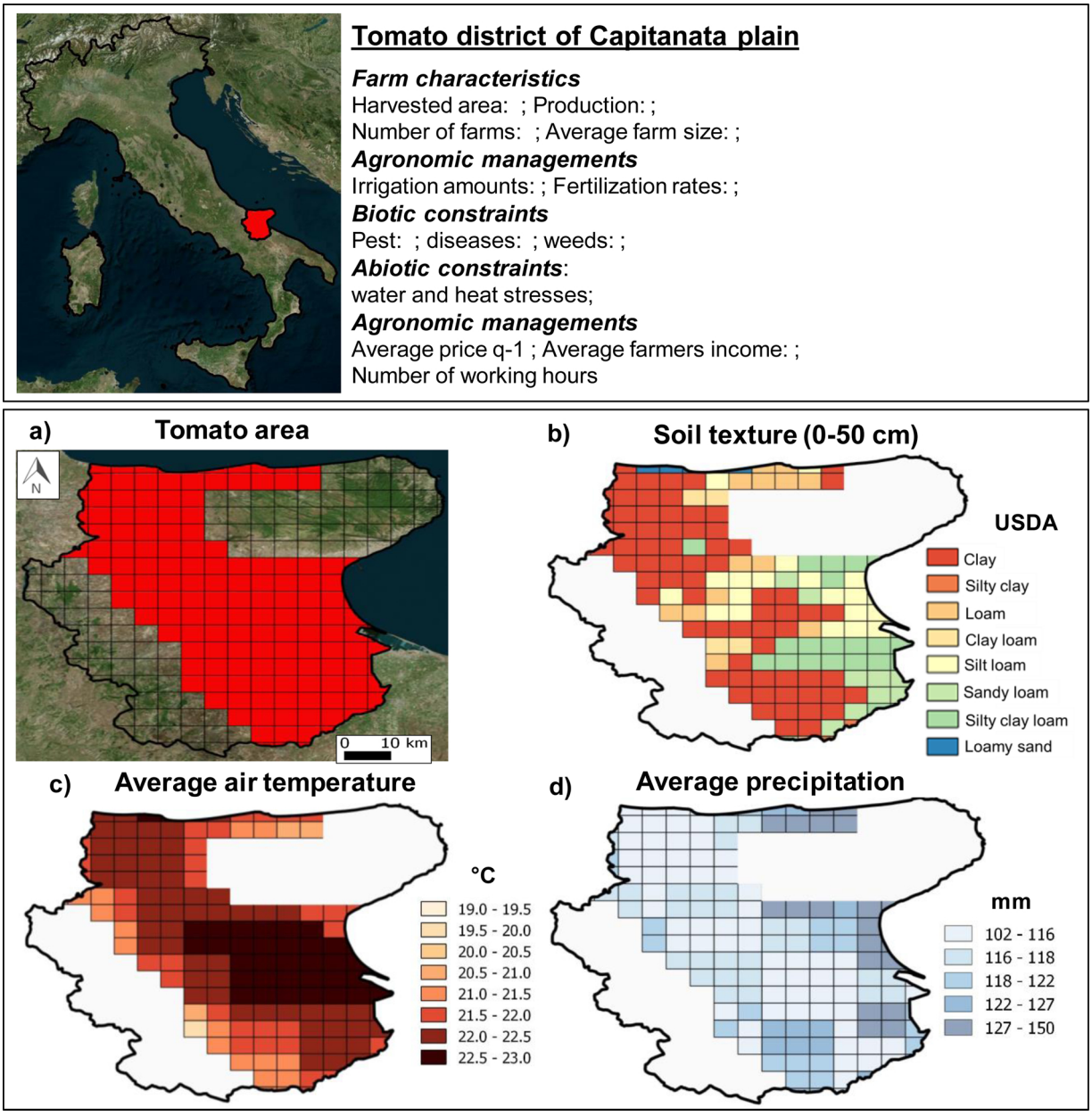

Fig. 2. Characterization of tomato cropping systems in the Capitanata plain, and input information used to perform spatially distributed simulations. a) tomato harvested area, b) soil texture in 0.5 m soil depth (USDA - Soil Survey Division Staff, 1993), c) average daily temperature (°C) and d) average cumulated precipitation (mm) during the cropping seasons (May-August) 1981–2010.

and ± 20% to evaluate its impacts on YQ and WP. The average transplanting date was derived from the field trials (4 May) and was changed by ± 1 and ± 2 weeks in the adaptation strategies. A Principal Components Analysis (PCA) was performed to summarise the performances of the simulated tomato growing systems under baseline and climate change conditions, considering the factorial combination of the adaptation strategies tested. We obtained Principal Components (PCs) on centred and scaled quantitative variables, through diagonalisation of the correlation matrix and extraction of the associated eigenvectors and eigenvalues. The variables 'fruit fresh yield', 'YQ',

Table 3
Synopsis of the adaptation strategies to climate change scenarios in Capitanata tested in the simulations. The total number of combinations of adaptation strategies in future simulation is 825. DI = deficit irrigation; ET_c = actual evapotranspiration (mm); DOY = day of year; *ref* = reference management practice in the study area.

DI regime (% ET_c)	Irrigation turn (days)	Cycle length (days)	Transplanting DOY
0, 10, 20,	6 *(ref.)*	93 *(ref.)*	124, May 4 *(ref.)*
30, 40,50,	9 *(+ 3 days)*	102 *(+10%)*	131, May 11 *(+1 week)*
60, 70, 80,	3 *(- 3 days)*	112 *(+20%)*	138, May 18 *(+2 weeks)*
90, 100		84 *(−10%)*	117, April 27 *(−1 week)*
(11 levels)		74 *(−20%)*	110, April 20 *(−2 weeks)*

'irrigation', 'total cycle length', 'brix', and 'water productivity' were set as active quantitative variables, *i.e.* used to compute PCs; the GCM, RCP, time frame, irrigation interval, cycle length and DI strategy were used as "supplementary" categorical variables, *i.e.* variables that were not used in the computation of PCs, and their coordinates were calculated as the barycenter of the corresponding simulations in the Principal Component space after the analysis. The FactoMineR R package was adopted to perform the analysis (Lê et al., 2008). The biplot was drawn using ggplot2 R Package (Wickham, 2009). A Hierarchical Clustering on Principal Components (HCPC) was then performed to detect any data structure and to characterize the impact of the adaptation strategies. The analysis was performed using function HCPC() of the FactoMineR package. η^2 was calculated for the active quantitative variables to measure the between-cluster variance associated with the extracted clusters and explained by each variable. We then characterised the Clusters with respect of quantitative and qualitative variables with a v-test. For quantitative variables, the cluster mean for variable X (x_q) was tested under the null hypothesis that the distribution of X was the same across Clusters (Eq. (4)).

$$u = \frac{\bar{x}_q - \bar{x}}{\sqrt{\frac{s^2}{n_q}\left(\frac{N-n_q}{N-1}\right)}} \quad (4)$$

where n_q is the number of simulations in cluster q, N the total number of genotypes, s the global standard deviation. The value of u is then compared to the corresponding quantile of the normal distribution; therefore, an absolute value higher than 1.96 indicate $p < 0.05$ and then a discriminating variable to describe the cluster; the sign indicates the direction of the difference from the global mean. For qualitative supplementary variables, the aim was to characterise the Clusters by investigating the frequencies of categorical variables within each cluster. A χ^2 test was at first performed between each categorical variable and the cluster variable. Frequencies N_{qj} (number of individuals of the group q in the category level j) of each level of the significant categorical variables were distributed as an hypergeometric distribution with the parameters N, n_j, $\frac{n_q}{N}$ (where n_j is the number of individuals that have taken the category j). The p-values were calculated and then transformed to the correspondent value in quantile of the Gaussian distribution with positive/negative sign indicating that the frequency of the category within the examined cluster is significantly higher/lower than the overall distribution. We performed these analyses using *catdes()* function of *FactoMineR* R package under R 3.2.3 environment (R Core Team, 2017).

3. Results

3.1. Model adequacy in reproducing current tomato growing systems

3.1.1. Model calibration and evaluation

The simulated dynamics of fruits fresh weight ($t\,ha^{-1}$), LAI ($m^2\,m^{-2}$), dry weight of plant organs ($g\,m^{-2}$) and soil water content ($m^3\,m^{-3}$) in the field trials carried out on 2017–2018 are shown in Fig. 3, along with measured field data and evaluation metrics computed for each DI regime tested.

TomGro_field correctly reproduced the measured dynamics of the plant variables considered in calibration under alternative DI regimes (Fig. 3), with MAE for phenological phases ranging from 3 days (S4) to 12.4 days for flowering (S2). Measured and simulated dynamics of fresh fruit weight within DI regime were similar in the two growing seasons, with TomGro_field simulating a steeper increase and a higher yield in 2018 in rainfed condition (DI_0), and an opposite situation under full irrigation (DI_{100}). The magnitude of increase in fresh fruits weight due to DI regimes was matched by the simulations, with the ratio between the average yields in DI_0 (37.9%) and DI_{75} – $DI_{75/50}$ (83.2%) with respect to DI_{100} close to field measurements (36.7% and 80.9%, respectively). The evaluation metrics confirmed the high accuracy of simulations across DI regimes (EF > 0.93), with MAE always below $60\,t\,ha^{-1}$ and RRMSE ranging from 21.4% (DI_0) to 31.7% (DI_{75}). Simulated LAI was higher in 2018 in all treatments except in DI_0 trials, coherently with measurements. TomGro_field matched the measured LAI dynamics, with a steeper increase in the post-transplanting phase and a peak at the end of June, ranging from 1.38 –1.4 $m^2\,m^{-2}$ in DI_0 to 2.1–2.35 $m^2\,m^{-2}$ in DI_{100}, followed by a smooth decline due to leaves senescence. The MAE was always lower than $0.26\,m^2\,m^{-2}$, with positive EF values (0.63–0.84) and RRMSE ranging between 37% in DI_{75} and 64.5% in DI_0. The model correctly simulated the increase in the dry weight of leaves and stems during the growing season, with 2018 leading to almost double dry weight in DI_{100} than in 2017. Corresponding model performances were positive, with RRMSE ranging between 25.7% in DI_{75} to 38.3% in DI_0, EF in the range 0.9 (DI_0) – 0.95 (DI_{75}) and MAE below $30\,g\,m^{-2}$. In spite of being excluded from calibration, the simulation of soil water content confirmed the accuracy of TomGro_field in reproducing the plant water uptake across DI regimes, with very low RRMSE (always below 7%) and positive EF (> 0.64). The model reproduced a steeper SWC decline in 2017 in DI_0, as well as the refilling of soil water content due to drip irrigation events occurred in the other DI regimes. After calibration, TomGro_field was evaluated using fresh fruit weight data collected in field experiments carried out in 2004–2015 to test the impact of alternative DI regimes on tomato production (Fig. 4). The model results in evaluation were positive, with the only exception of 2015 where simulations showed a clear underestimation of fresh fruits weight in DI_{75} and DI_{100}. In all the other years, the model errors were lower, with RRMSE ranging from 6.7% in 2016 (DI_{75} and DI_{100}) to 20.7% in 2013 (DI_0, DI_{50}, DI_{75} and DI_{100}).

The accuracy in simulating phenological development and water dynamics in the soil-plant system laid the foundation for an accurate simulation of tomato fruit quality. The comparison between measured and simulated DB is presented as scatterplots in the supplementary material (Appendix F, Fig. F.1). TomGro_field succeeded in reproducing DB at the end of the season, with slightly better results in calibration (RRMSE = 5.46%, MAE = 0.24°Brix, EF = 0.82 and R^2 = 0.82) than in evaluation (RRMSE = 6.92%, MAE = 0.29° Brix, EF = 0.71 and R^2 = 0.72). Although the model accurately reproduced the response of fruit quality to different DI regimes, a saturation effect was observed at full irrigation regime (DI_{100}), with an underestimation of DB in five cases out of eight.

3.1.2. Model application in Capitanata area

The spatially distributed application of TomGro_field in the tomato areas in Capitanata is presented in Fig. 5, using baseline conditions as input. Simulations were performed using eleven DI regimes, ranging from DI_0 to DI_{100} using a 10% ET_c interval. The same geographic area was then adopted to perform the simulations under climate change scenarios.

The simulated fruit yield under rainfed conditions reached peaks of 16-18 $t\,ha^{-1}$ in the eastern part and lowest production in the western areas. The increase in the supply of irrigation water increased tomato yield up to 51-54 $t\,ha^{-1}$ in DI_{50} and 94-110 $t\,ha^{-1}$ in DI_{100} and highlighted a north-south decreasing gradient in tomato fruit production (Fig. 5). The simulation of fruit quality revealed an opposite pattern, with highest DB values (7.6–7.8 °Brix) in the lowest yielding areas under D_0 regime; conversely, the lowest DB data (4.0–4.1 °Brix) were obtained in the top producing areas of DI_{100}. YQ showed similar geographical patterns than fruits yield, although with smoothed differences across the simulated area (Fig. 5). The amount of irrigation water almost reflected the spatial patterns of annual rainfall and varied in the range 515–540 mm under full irrigation (DI_{100}), with highest values in the north-west and in the central parts of Capitanata, *i.e.* the drier and warmer zones (Fig. 2).

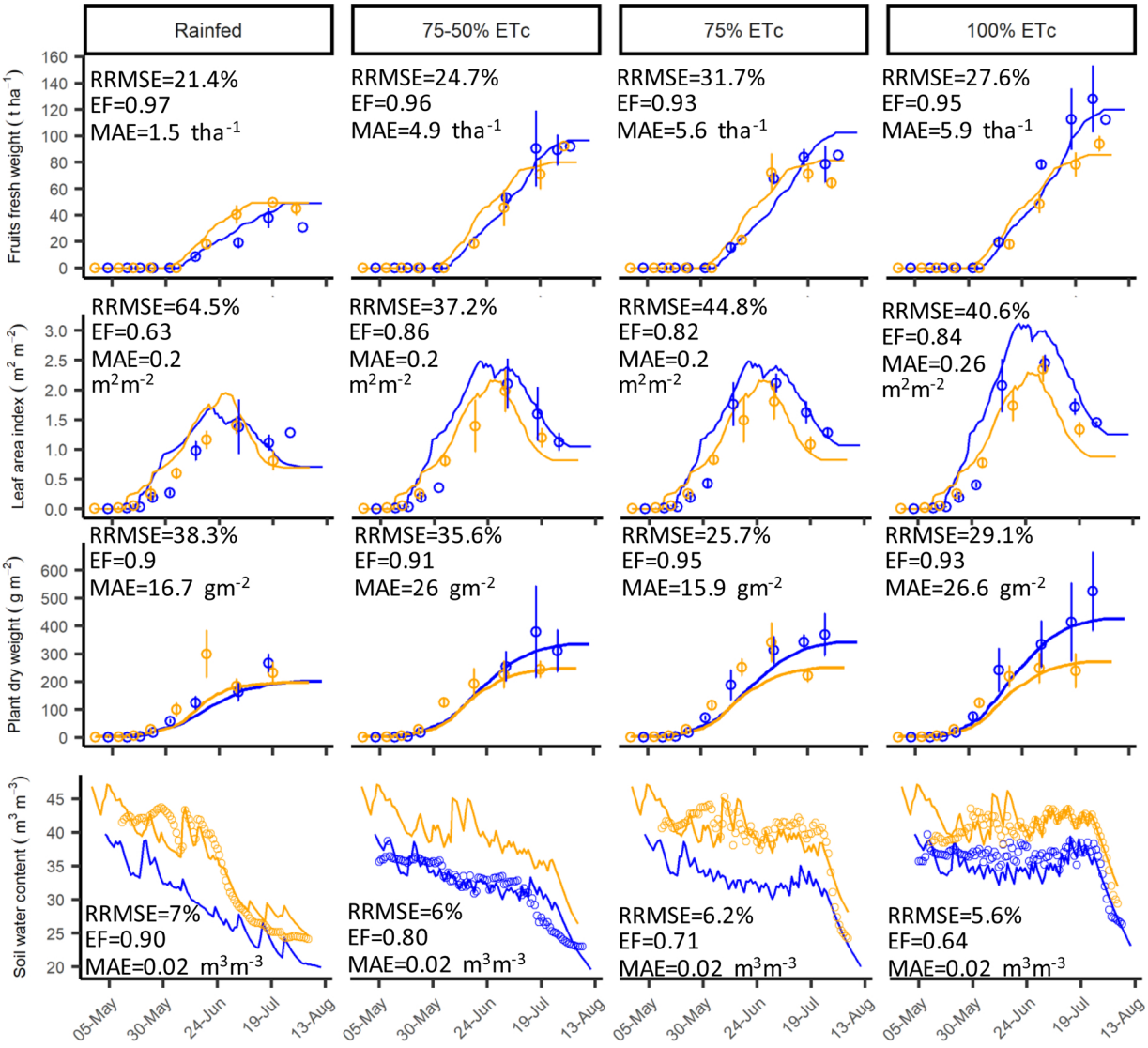

Fig. 3. Model performances in reproducing the experimental trials used in calibration in 2017 (blue) and 2018 (orange). The evaluation metrics computed on the different deficit irrigation regimes (columns) are reported in the plots; they are the relative root mean square error (RRMSE), the modeling efficiency (EF) and the mean absolute error (MAE). Model calibration focused on fruits fresh weight ($t\,ha^{-1}$), leaf area index ($m^2\,m^{-2}$), and plant dry weight ($g\,m^{-2}$). The dynamics of simulated and measured soil water content ($m^3\,m^{-3}$) are also reported in the bottom row of plots. Simulated data are indicated by lines, measured data by points with error bars corresponding to the standard deviation in field samplings. (For interpretation of the references to colour in this figure legend, the reader is referred to the web version of this article).

3.2. Future trends in tomato productions

The YQ distribution in future weather scenarios (5 time frames, 2030–2070), considering the two RCPs (2.6 and 8.5), the four GCMs (GISS, HADGEM, MIROC and NORESM) and different irrigation strategies (eleven, from DI_0 to DI_{100}) are shown as boxplots in Fig. 6, along with average YQ simulated in baseline conditions (horizontal red line). The simulated variability is generated by the spatial application of the model in the Capitanata plain (152 cells), and by the 20 years considered for each combination of GCM × RCP × time frame × DI regime.

The projected impacts of climate change without adaptation are generally negative on tomato production and fruit quality. The average YQ reductions in all DI strategies varied according to the different GCMs in the range −5.02% (GISS) and −10.84% (MIROC). These simulations did not reveal any clear time trend, as the average reductions compared to baseline conditions were constant across time frames, and ranged between −6.2% (2050) and −8.1% (2040). The simulated YQ according to the two extreme RCPs led to a similar yield decrease with respect to baseline (about −7%). Major differences between current and future simulations emerged across DI strategies: while YQ simulated under $DI < DI_{30}$ was higher in future simulations than in baseline conditions (+9.3%), YQ reductions (−12%) were simulated in the intermediate DI regimes ($> DI_{30}$, $< DI_{70}$). We focused the analysis on the DI regimes equal or higher than DI_{50}, assumed as the minimum water amount used by tomato growers in current conditions. The average relative changes (%) of irrigation amounts (mm), fruits yield ($t\,ha^{-1}$), YQ ($t\,ha^{-1}$) and WP ($kg\,m^{-3}$) in 2030 and 2070 compared to baseline (absolute values) are reported in Table 4.

Simulation results showed very limited variations in the current and future irrigation amounts, the former ranging from 263 mm (DI_{50}) to 506 mm (DI_{100}). The simulated WP ranged between 13.2 $kg\,m^{-3}$ (DI_{100}) and 15.3 $kg\,m^{-3}$ (DI_{60} and DI_{70}) in baseline conditions, with fruits weight comprised between 50.6 $t\,ha^{-1}$ (DI_{50}) and 96.2 $t\,ha^{-1}$ (DI_{100}). YQ (DI_{50} = −13%; DI_{100} = −8%) showed lower variability than fruits weight at low DI regimes (DI_{50} = −16%; DI_{100} = −8%) because of the positive impacts of low irrigation amounts on DB. In the same conditions, the simulated tomato systems obtained similar

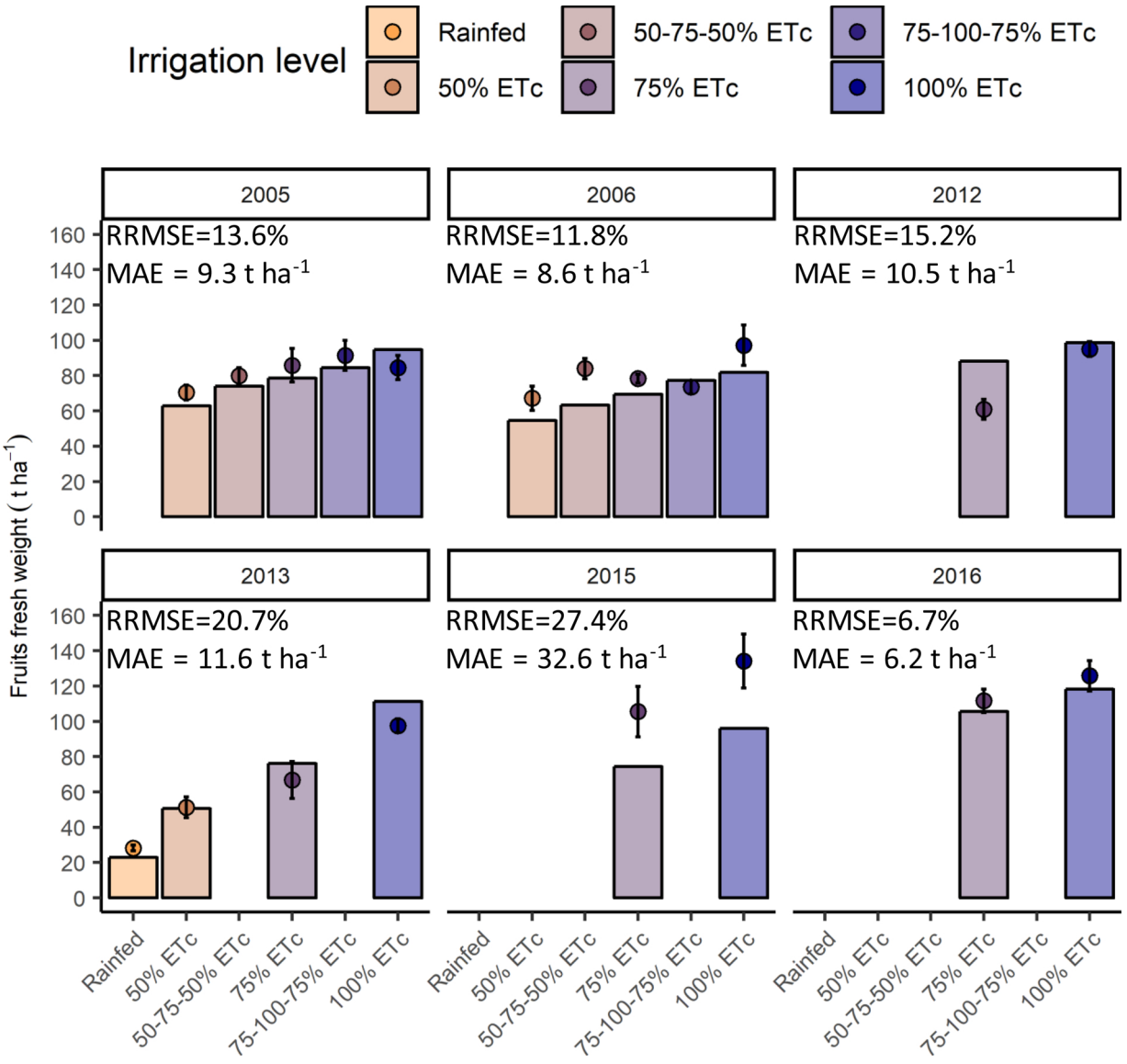

Fig. 4. Model performances in reproducing fruits fresh weight in the field trials used for independent evaluation. The evaluation metrics computed for each experimental year are reported on the plots; these are the relative root mean square error (RRMSE, %) and the mean absolute error (MAE, t ha^{-1}). The measured data under the various deficit irrigation strategies (gradient of colors from red, rainfed, to full irrigation, blue) are plotted as points with error bars corresponding to standard deviation, whereas bars correspond to the simulated data. (For interpretation of the references to colour in this figure legend, the reader is referred to the web version of this article).

performance across time frames (2030–2070), with a larger reduction of WP (9% in 2030, 11% in 2070), fresh fruits weight (16% in 2030, 17% in 2070) and YQ (13% in 2030 and 2070) at low DI regimes, especially in DI_{50}. The lowering of the performances was less marked under DI_{100}, with relative changes with respect to baseline always smaller than -10% for all the indicators considered, and large similarities between 2030 and 2070.

3.3. Identifying sustainable irrigation strategies

PCA was performed to summarise the data using a multivariate approach and simultaneously consider all the indicators of tomato growing systems performances, *i.e.*, the fresh fruit yield, DB, total cycle length, YQ, irrigation amounts and WP. We considered the first two components for interpretation, explaining 87.6% of the total variance. The correlation coefficients were calculated between the Principal Components (PCs) and each simulated and categorical variable (Table 5) and the associated *p*-values ($\alpha = 0.05$) computed to rank the variables according to their relevance.

The first component (PC1) accounted for 61.8% of total variance and summarised all the quantitative variables, with correlations ranging from 0.48 (DB) to 0.98 (YQ) and suggesting a high degree of multicollinearity (Table 5). Simulations performed with $DI \geq DI_{80}$ and adopting varieties with longer cycle length (+10, +20%) were at positive coordinates on PC1; these were opposed, at negative coordinates, by simulations with short cycle varieties (−10%; −20%) and lower irrigation rates (Fig. 7a). MIROC confirmed to be the worst-case scenario (Appendix G), as its barycenter was at significant negative coordinate on this axis (-0.32) thus suggesting an adverse effect mainly on YQ. The other GCM × RCP combinations showed a negligible effect on the variability of outputs as their barycenters were at coordinates slightly different from zero.

The second Principal Component (PC2) explained 25.8% of the total variance (Table 5) and was positively correlated with DB and total cycle length, and negatively with all the other variables (YQ, Yield, Irrigation, WP). This structure summarised an inverse correlation, *i.e.* higher

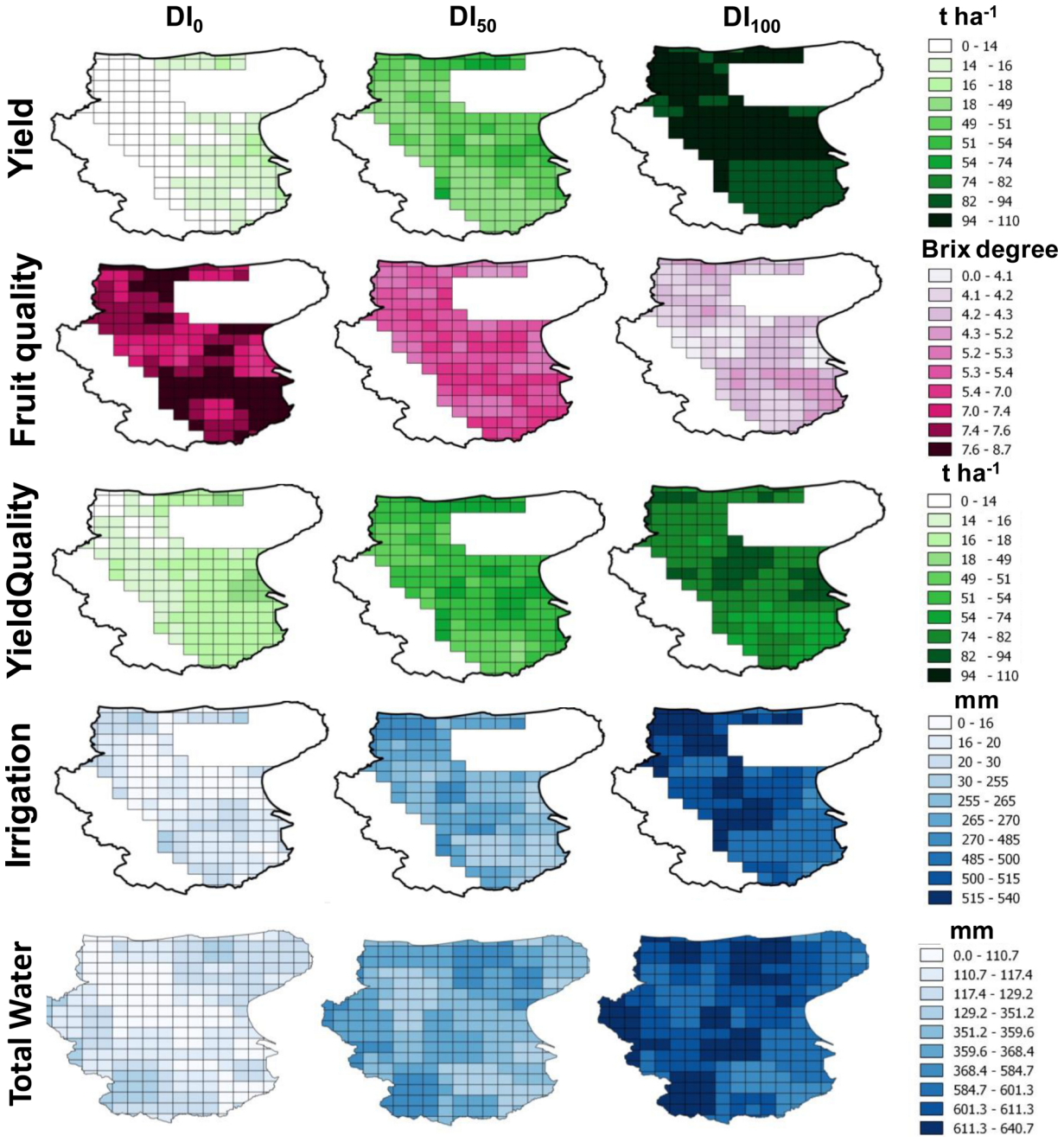

Fig. 5. Spatially distributed simulations of fresh fruit yield (Yield, t ha^{-1}), fruit quality (°Brix), YieldQuality (t ha^{-1}, please see text) and irrigation amount (Irrigation, mm) in Capitanata under baseline scenario. Results are presented as the average of the values simulated at the end of the season in the period 1981–2010 for the three deficit irrigation regimes DI_0, DI_{50}, DI_{100}.

DB associated with longer cycle length but with lower yields and WP (Fig. 7a). The supplementary categorical variables were correlated with PC2 similarly to PC1 (Table 5); even in this case, MIROC was the only GCM meaningfully associated with this PC (0.21), indicating an increased DB and reduced WP but lower Yield (Appendix G). RCP and time frame affirmed again to have low impact on the variability of outputs. Along PC2, simulations performed with DI < DI_{70} and varieties with standard or long cycle (0% − +20%) were at positive coordinates. A hierarchical clustering algorithm was applied on the extracted PCs (Hierarchical Clustering on Principal Components, HCPC) to detect any inner structure in the data and to provide an overview of the performances of the different adaptation strategies. Six clusters were selected to maximise the relative loss of inertia. The data plotted in PCs space, colour-coded by cluster are presented in Fig. 7b. The obtained partition was characterised referring to the original qualitative and quantitative variables, using an alpha level $\alpha = 0.05$ for all the statistical tests.

The six clusters defined in the PC biplot (Fig. 7b), showed a clear distinction between the simulations performed with variable cycle length, and a horizontal gradient corresponding to alternative DI regimes. The complete characterization of the six clusters is provided in Appendix G. The other adaptation strategies did not reveal any clear pattern within the clusters, as well as the different combinations of RCP, GCM and time frames, as already discussed in the PCA results. The amount of variance between-clusters explained by each of the original variables was assessed by calculating η^2, revealing that all the variables except water productivity ($\eta^2 = 0.58$) explained a comparable amount of the variability among clusters ($0.71 < \eta^2 > 0.85$). Cluster 1 (C1) and

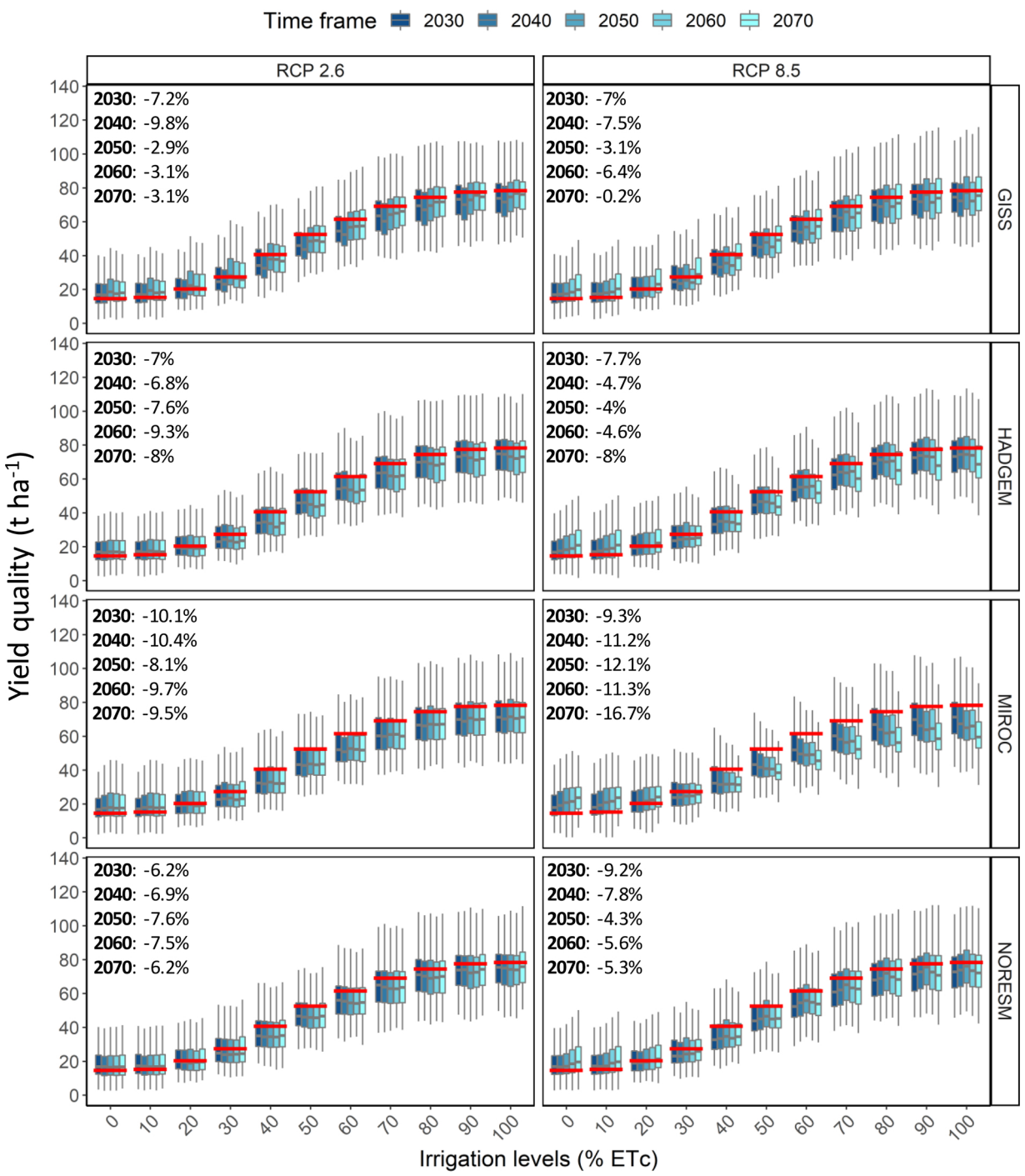

Fig. 6. Simulated data of yield quality (t ha^{-1}) in future simulations without the implementation of adaptation strategies. Simulation results correspond to the two Representative Concentration Pathways (RCP, columns) 2.6 and 8.5 (columns), the four GCMs (GISS, HADGEM, MIROC, NORESM, rows), and the five time frames (2030–2070). They are reported for the eleven deficit irrigation regimes (x-axis, from rainfed to full irrigation). The boxplots correspond to the variability in the 20 years of simulations and in the 152 cells covering the tomato harvested area in Capitanata.

Cluster 3 (C3) were similar in their composition and presented simulations performed with low irrigation amounts, with main differences in the duration of crop cycle. C1 comprised tomato varieties with shorter cycle length (−10% and −20%, mean simulated growing season = 74.5 days), whereas C3 grouped simulations in which the duration of phenological phases was equal or greater (+10%, +20%, simulated growing season = 93 days) than the standard cv. Ulisse. The main adaptation strategies characterising these two clusters combined a DI regime below DI_{70} (83% in C1, 89.7% in C3), shorter irrigation interval (3 days, 45% in C1 and 54.9% in C3) and postponed transplanting dates (May 18 = 24.9% in C1 and 30.4% in C3). The average irrigation amounts in these clusters were significantly lower than the overall mean (249 mm in C1 and 310 mm in C3, overall mean = 377 mm), which were associated to poor performances both in terms of YQ (34 t ha^{-1} in C1 and 45.2 t ha^{-1} in C2) and WP (11 kg m^{-3} in C1 and 11.5 kg m^{-3} in C2). Cluster 2 (C2) was mainly composed by earlier tomato varieties than the cv. Ulisse (−20%, 66.8% of simulations, length = 73.3 days), and DI_{80} (31%) and DI_{70} (23.7%), with long irrigation interval (9 days, 39.2%) and anticipated transplanting date (April 27, 41%). The average YQ in this cluster was lower than the

Table 4
Performances of the simulated tomato growing systems under baseline and future conditions in 2030 and 2070, considering deficit irrigation regimes above 50% of crop evapotranspiration (ET_c). Average values are reported for each time frame considered, with absolute values for the baseline and relative change for the future conditions. Irr. = irrigation water, Y = fresh fruits weight; YQ = yield quality, WP = water productivity.

Deficit irrigation	Baseline				2030				2070			
% ET_c	Irr. mm	Y t ha^{-1}	YQ t ha^{-1}	WP kg m^{-3}	Irr. % with respect to baseline	Y	YQ	WP	Irr. % with respect to baseline	Y	YQ	WP
50	263	50.6	53.5	14.9	0	−16	−13	−9	−1	−17	−13	−11
60	312	65.2	62.4	15.3	1	−14	−11	−8	0	−15	−12	−11
70	360	79.2	69.9	15.3	1	−12	−9	−7	1	−12	−10	−9
80	409	90.2	75.4	14.9	1	−10	−8	−6	1	−10	−9	−9
90	457	95.0	78.5	14.2	1	−8	−8	−6	1	−10	−9	−9
100	506	96.2	79.5	13.2	1	−8	−8	−6	2	−9	−9	−9

Table 5
Correlation coefficients between simulated variables and the first two Principal Components (PC) with an indication about the significance of differences from 0, and the amount of variance explained by each PC. Significance codes: *** = $p < 0.001$, ^{ns} = not significant. The PCs were computed using 21,606 simulations as input data.

Variable	PC1	PC2
Quantitative active variables		
Fresh fruit yield	0.83***	−0.53***
Degree Brix	0.48***	0.87***
Total cycle length	0.75***	0.63***
Yield quality (YQ)	0.98***	−0.15***
Irrigation	0.84***	−0.12***
Water productivity	0.74***	−0.28***
Qualitative categorical variables		
Deficit irrigation regime	0.32***	0.37***
Shift in cycle length	0.51***	0.48***
Transplanting date	0.08***	0.03***
GCM	0.005***	0.005***
RCP	$< 10^{-5\ ns}$	$< 10^{-5ns}$
Time frame	$< 10^{-5\ ns}$	$< 10^{-5\ ns}$
Irrigation interval	0.004***	0.009***
Explained variance	61.8%	25.8%

average (55.8 t ha^{-1} *vs.* 65.3 t ha^{-1}), mainly due to low DB ($\bar{X}_{C2}$ = 4°Brix) associated with good levels of average fresh fruit yield (67.7 t ha^{-1}) and irrigation amounts lower than the average ($\bar{X}_{C2}$ = 328 mm). The best performances of the simulated tomato growing systems were grouped in clusters 4 (C4), 5 (C5) and 6 (C6), despite main differences in the adaptation strategies implemented. C4 grouped simulations performed with standard (59.7%) or short-duration cultivars (-10%; 35.1% of the simulations), and DI_{80} (18.1%), DI_{90} (36%) and DI_{100} (37.6%). The main irrigation intervals in this cluster were 6 days (35.4%) and 9 days (35.3%). The corresponding mean YQ was slightly higher than the average (69.1 t ha^{-1}), due to high fresh fruit weight ($\bar{X}_{C4}$ = 80.6 t ha^{-1}) but low brix values ($\bar{X}_{C4}$ = 4.1), determined by large irrigation amounts (444 mm, water footprint = 13.4 kg m^{-3}). The main adaptation strategies characterizing C5 and C6 were the adoption of varieties with longer cycle length than the cv. Ulisse (simulated growing season = 96 days in C5 and 101 days in C6) coupled with an anticipated transplanting date, whereas they differed in the DI regimes. C5 grouped simulations performed according to an overall water saving strategy (DI_{50} = 15.6%, DI_{60} = 33.9%, DI_{70} = 30.8%), adopting varieties with longer cycle length (+10% = 41.9%; +20% = 38.6%), an anticipated transplanting date (April 20 = 38.5%, April 27 = 14%) and a short-medium irrigation interval (3 and 6 days = 52.4%). The resulting average YQ was significantly higher than the average (70.8 t ha^{-1}), with high DB (6.3°Brix) and average irrigation amounts of 367.6 mm (average WP = 15.6 kg m^{-3}). Finally, C6 grouped simulations performed with DI ≥ 80% ET_c (DI_{80} = 25.9%, DI_{90} = 31.2%, DI_{100} = 32.3%), longer cycle length (+10% = 46.3%, +20% = 52.7%) and anticipated transplanting date (April 20 = 47.3%, April 27 = 20.2%), with mostly 3 days (37.1%) and 6 days (36.8%) of irrigation interval. This cluster corresponded to the highest average YQ (93.1 t ha^{-1}), with favorable DB (6.1°Brix) and amounts of fresh fruit yield (104.4 t ha^{-1}, WP = 17.2 kg m^{-3}), although associated with large irrigation volumes (516 mm).

4. Discussion

4.1. Rationale for model development

This work fits into the context of the many research activities which have been developed in recent years to sustain tomato yields in Mediterranean area through simulation modeling. The common purpose of these studies is to foster the strategic design of the future tomato growing systems considering the expected increased frequency, duration and intensity of heat stress and drought events, which could dramatically reduce the stocks of water resources in the upcoming years (Ronco et al., 2017). Our methodological approach has some peculiarities with respect to available literature, the main ones represented by i) the use of a specific model targeting both quantitative and qualitative aspects of tomato yield, ii) its calibration with data collected in dedicated field trials and the subsequent evaluation on an independent dataset of long-term experiments, and iii) the evaluation of the future yield trends of simulated tomato growing systems according to alternative adaptation strategies, which were derived according to local-based knowledge. A new tomato simulator, TomGro_field, has been derived from the original TOMGRO greenhouse model (Jones et al., 1991) with the purpose of accounting for the impact of soil water availability during crop growth, with a feedback on the qualitative aspects of tomato productions, synthesized by the DB (Chen et al., 2008). Acutis et al. (2009) forced the STAMINA model (Acutis et al., 2007) with leaf area index data from a Geographic Information System to develop a decision support system to schedule tomato irrigation in Capitanata plain. Rinaldi et al. (2011) calibrated and evaluated the AquaCrop model (Raes et al., 2009) for tomato crop with field data, and applied it on a long-term simulation experiment to evaluate the agronomic and economic performance of alternative management scenarios. Ventrella et al. (2017) used the CROPGRO model (Scholberg et al., 1987) in order to estimate the green and blue water (BW; crop evapotranspiration deriving from irrigation) requirements of industrial tomato under alternative climate change scenarios towards the optimization of water use efficiency. Our rationale implied the definition of a new model for open field tomato aiming at reproducing the underlying system using an approach specifically developed to simulate the target crop. TomGro_field provides a detailed representation of the plant growth and phenological development (Boote et al., 2012), while simplifying the definition of the crop parameters needed for its initialization. The impact of soil water availability on crop growth is a central topic in this work, borrowed from the management-oriented

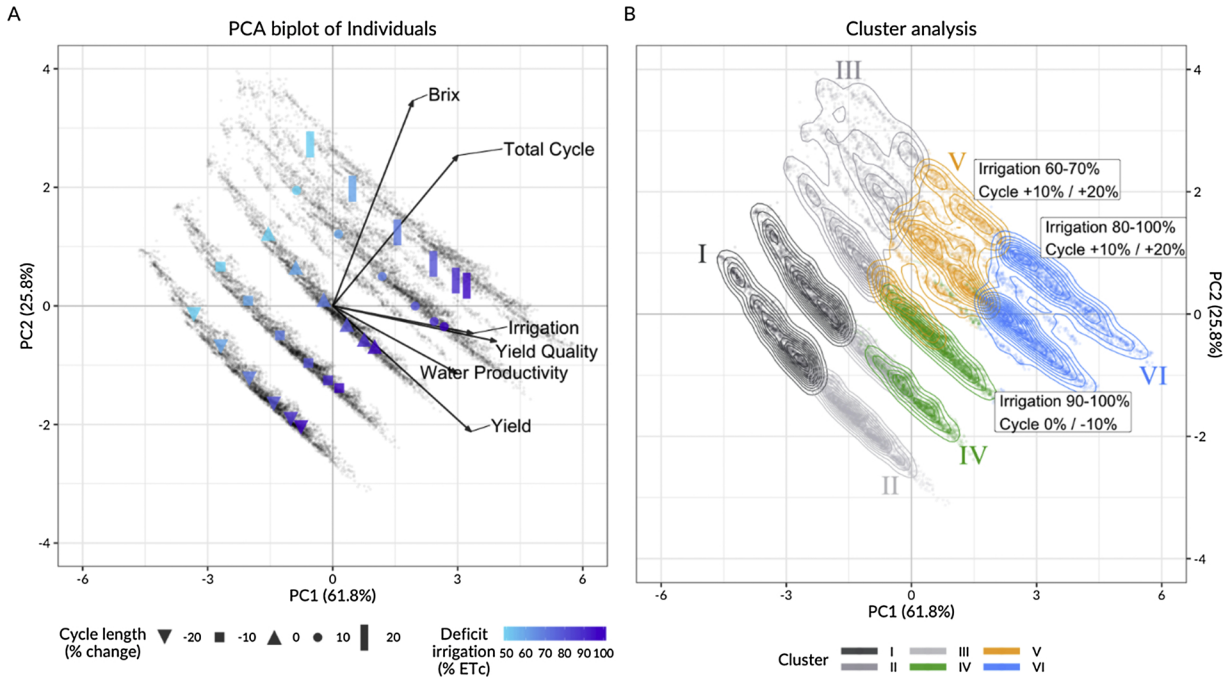

Fig. 7. A – PCA biplot of individuals combined with variables. Each grayscale point corresponds to one out 21,606 simulations. Colored points show the barycenters of the combined categorical variables 'Cycle length' (shape) and 'Deficit irrigation' (blue tone). B – PCA biplot with points color-coded according to cluster classification; clusters with the most promising strategies influencing Water Productivity and Yield Quality were labeled to summarise the most frequent categories of 'Deficit Irrigation' and 'Shift in cycle length' within the Cluster. (For interpretation of the references to colour in this figure legend, the reader is referred to the web version of this article).

CropSyst model (Stockle et al., 1999), which has been extensively used to assess the impact of alternative irrigation practices in cereals (*e.g.*, maize, Nana et al., 2014) and industrial crops (tomato, Onofri et al., 2009; potato, Montoya et al., 2018). The simulation of crop evapotranspiration, which drives the plant demand in our simulations, is based on leaf and soil critical water potential, as parameterized by Onofri et al. (2009), which applied the same model on tomato systems in Perugia, Central Italy. We provide here a new function to simulate the qualitative aspects of tomato fruits using DB as a proxy of fruit quality. The new model considers the beneficial effects of moderate water stress conditions during ripening phase on tomato quality (Chen et al., 2008), and demonstrated to be capable of capturing DB variability measured in the field experiments. The evaluation metrics used to quantify the model accuracy in reproducing field reference data in calibration and evaluation, as well as the results of spatialized spatially-distributed simulations, proved the adequacy of TomGro_field in characterizing the impact of alternative DI regimes. Moreover, the availability of a modular version of the seminal TOMGRO model (Louski et al., 2013) simplified the transfer of model source code into the BioMA platform, whose architecture proved to maximize the reusability and extendibility of agricultural system models, while fostering the substitution of process models with alternative options facilitating the contribution from domain specialists (Donatelli et al., 2014). The BioMA implementation eased model application to other tomato districts, *i.e.* with different agro-climatic conditions and cultivars. Such an application in other areas and/or to other varieties should be preceded by a novel calibration of phenology, growth, soil water and fruit quality modules, in turns requiring multi-year and multi-variable field data collection under contrasting pedo-climatic conditions.

4.2. Future trends in tomato production

In this study, the future simulations with no agronomic adaptation indicate an overall decrease of tomato yield and quality with respect to current conditions. These results agree with previous studies, despite we obtained smaller yield reductions than in Ventrella et al. (2017), who reported 20% tomato yield decrease in the same area. In that study, the simulated BW and BW requirement (i.e. the ratio between BW and yield) in the future increased up to 30% and 40% respectively compared to the baseline. The differences with respect to our study include the crop model used, the time period considered (2070–2099), the management strategy tested and the climatic projections, which were characterized by a very large temperature increase (average +5 °C, IPCC SRES AR4). Despite the decrease in irrigation water use efficiency projected by Ventrella et al. (2017) was approximately four times higher than our simulations, the differences between the two studies decreases when comparable scenarios were considered (*i.e.* RCPs AR5 MIROC_8.5 versus SRES AR4 A5), due to the marked similarity in temperature (+5/6 °C on average) and precipitation (up to -40% decline) projections. Our future climatic scenarios were derived by the factorial combination of two extreme RCPs and four GCMs, which were the same adopted in Bregaglio et al. (2017), and five time frames (decades from 2030 to 2070). The resulting ensemble of climatic projections did not explore the whole variability in terms of plausible future climatic predictions, despite the four GCMs chosen in this study were widely used in crop modeling studies (Burke et al., 2015) and grouped in separate clusters according to temperature and precipitation data (Zubler et al., 2016), with GISS and NorESM presenting the largest dissimilarity.

4.3. Adaptation to climate change scenarios

The fundamental message emerging from the test of alternative DI strategies, variable cycle length, and shifts in transplanting dates is that farmer management will be a key factor for the future sustainability of the tomato sector in the Mediterranean area. We identified a spectrum of candidate adaptation strategies capable to preserve the competitiveness and sustainability of the tomato growing systems. PCA suggested that the performances of tomato growing systems were mostly affected by the DI regime and by the cycle length, followed by the

transplanting date and the irrigation interval. DI regimes have been successfully tested as valuable strategies in dry regions where water is the main limiting factor to crop cultivation (English, 1990; Fereres and Soriano, 2007). The most promising strategies to optimize tomato yield and quality in the future will be the application of moderate DI regimes (DI_{60}-DI_{70}) on tomato varieties with long cycle length (+10%, +20% with respect to cv. Ulisse), that should be transplanted early (20–27 April). The simulated increase in the amount of irrigation water (DI_{80}-DI_{100}) led to benefits for tomato yield levels, while requiring larger irrigation amounts than in current conditions, contrarily to the projected restriction in groundwater availability. Our results are limited to the agronomic management, and should be integrated by a multi-actor, socio-economic analysis involving public and private stakeholders. Such a research project should target the analysis of the future trends in water availability and tomato prices, explicitly considering the cost of farmer inputs (*i.e.* seed, fuel, water, and fertilizers). Additional efforts are needed for the purpose, as well as further developments of TomGro_field to account for the effect of fertilization and of other qualitative aspects of tomato productions (fruit color, firmness and titratable acidity). Another aspect that needs further evaluation is the assessment of the sensitivity of the new TomGro_field model to parameter changes. There is a limited literature on this topic, mostly focused on a simplified version of the original TomGro model (Vazquez-Cruz et al., 2014), and on the outputs uncertainty as a function of variable environmental conditions (Cooman and Schrevens, 2004; Dimokas et al., 2012). Our rationale here has been (i) to set the majority of the parameters according to their literature values (77% of the total number), then (i) to maximize the number of parameters which could have been effectively measured in the field experiments (13% of the total number), while limiting the automatic calibration to the remaining parameters (10% of the total number). This choice was driven by the need to carry out a complex workflow from beginning to end, constituted by the model calibration with detailed field experiments, the model evaluation with historical datasets, the application of the model under a set of climate change scenarios and finally the identification of the best adaptation strategies to sustain tomato cultivation in the area of interest. The execution of a robust assessment of the model sensitivity, which would include all the parameters of the new TomGro_field model and its application in contrasting pedo-environmental conditions, would deserve a dedicated scientific paper. Such a work will be of major interest in light of the spatialized application of the model over large areas, because it will allow selecting the parameters on which a user has to focus during calibration, especially in situations where a limited set of field experiments is available, differently from the modelling work presented here.

5. Conclusions

We conducted a crop modeling study to assess the performances of current and future tomato growing systems in Capitanata, considering basic farmers adaptation strategies under an ensemble of climate change scenarios. The main innovation in our rationale is the development of a model specific for open field tomato considering the beneficial effects of moderate water stress during ripening phase on fruit quality, which demonstrated to reproduce the data collected in field conditions. Relative to the future trends in tomato production, the simulations with no agronomic adaptation indicate an overall decrease of tomato yield and quality with respect to current situation. The farmer management emerged as the key factor to foster the future sustainability of the tomato sector in the Mediterranean area, by means of alternative DI strategies, variable cycle length, and shifts in transplanting dates. The most promising strategies to optimize tomato yield and quality in the future will be the application of moderate deficit irrigation regimes (DI_{60}-DI_{70}) on tomato varieties with longer cycle length and the anticipation of 1–2 weeks in transplanting dates.

Our simulations envisaged the potential of the Capitanata plain to continue sustaining the Italian tomato production, and identified the most promising strategies to improve irrigation water use. These basic agronomic practices could now be considered by tomato growers in the area, as well as by the public bodies in charge of designing the future tomato systems.

Acknowledgements

This research was supported by the AgriDigit-Agromodelli project (DM n. 36502 of 20/12/2018), funded by the Italian Ministry of Agricultural, Food and Forestry Policies and Tourism. We would like to show our gratitude to prof. Raphael Linker and Dr. Marc Lousky, Israel Institute of Technology, for sharing their C# implementation of the TOMGRO model and to Dr. Eugenio Nardella for his skillful technical assistance during the experimental trials.

Appendix A. Supplementary data

Supplementary material related to this article can be found, in the online version, at doi:https://doi.org/10.1016/j.eja.2019.125937.

References

Acock, B., Charles-Edwards, D.A., Fitter, D.J., Hand, D.W., Ludwig, L.J., Wilson, J.W., Withers, A.C., 1978. The contribution of leaves from different levels within a tomato crop to canopy net photosynthesis: an experimental examination of two canopy models. J. Exp. Bot. 29, 815–827.

Acutis, M., Confalonieri, R., 2006. Optimization algorithms for calibrating cropping systems simulation models. Bibliotheca Fragmenta Agronomica 11, 259–260.

Acutis, M., Rana, G., Trevisiol, P., Bechini, L., Laudato, M., Ferrara, R.M., Richter, G.M., 2007. Integrating a spatial micrometeorological model into the risk assess-ment for arable crops in hilly terrain. In: Kersebaum, K.C., Hecker, J.M., Mirschel, W., Wegehenkel, M. (Eds.), Modeling Water and Nutrient Dynamics in Soil-Crop Systems. Springer.

Acutis, M., Rinaldi, M., Fumagalli, M., Perego, A., 2009. Integration of a crop simulation model and remote sensing information. In: Cao, W., White, J.W., Wang, E. (Eds.), Crop Modeling and Decision Support. Springer, Berlin, Heidelberg.

Allen, R.G., Jensen, M.E., Wright, J.L., Burman, R.D., 1989. Operational estimate of reference evapotranspiration. Agron. J. 81, 650–662.

Asseng, et al., 2015. Crop Modeling for Climate Change Impact and Adaptation. Chapter 20. https://www.sciencedirect.com/science/article/pii/B9780124171046000200.

Beveridge, 2018. Beveridge. https://link.springer.com/content/pdf/10.1007%2Fs10584-018-2160-z.pdf.

Boote, K.J., Rybak, M.R., Scholberg, J.M.S., Jones, J.W., 2012. Improving the CROPGRO-Tomato model for predicting growth and yield response to temperature. Hort. Sci. 47, 1038–1049 ISSN 0018-5345.

Bregaglio, S., Hossard, L., Cappelli, G., Resmond, R., Bocchi, S., Barbier, J.-M., Ruget, F., Delmotte, S., 2017. Identifying trends and associated uncertainties in potential rice production under climate change in Mediterranean areas. Agric. Forest Meteorol. 237, 219–232. https://doi.org/10.1016/j.agrformet.2017.02.015.

Burke, M., Dykema, J., Lobell, D.B., Miguel, E., Satyanath, S., 2015. Incorporating climate uncertainty into estimates of climate change impacts. Rev. Econ. Stat. 97, 461–471. https://doi.org/10.1162/REST_a_00478.

Cahn, M.D., Herrero, E.V., Hanson, B.R., Hartz, T.K., Miyao, E.M., 2001. Water management strategies for improving fruit quality of drip irrigated processing tomatoes. Acta Hort. 542, 111–116.

Cantore, V., Sergio, L., Di Venere, D., Schiattone, M.I., Boari, F., 2016. Effect of pyraclostrobin on tomato crop under salinity stress. In: Proceedings of International Conference 'IrriMed 2015'. Valenzano (Bari, Italy). pp. 154–155.

Cappelli, G., Pagani, V., Zanzi, A., Confalonieri, R., Romani, M., Feccia, S., Pagani, M.A., Bregaglio, S., 2018. GLORIFY: a new forecasting system for rice grain quality in Northern Italy. Eur. J. Agron. 97, 70–80.

Challinor, 2013. Improving the Use of Crop Models for Risk Assessment and Climate Change Adaptation. https://www.ncbi.nlm.nih.gov/pmc/articles/PMC5738966/.

Chen, L., Raghavan, G.S.V., Charlebois, D., Charles, M.T., Vigneault, C., 2008. Non-destructive measurement of tomato quality using visible and near-infrared reflectancece spectroscopy. Canadian Soc. Bioeng. 8 (197), 1–15.

Collins, W.J., Bellouin, N., Doutriaux-Boucher, M., Gedney, N., Halloran, P., Hinton, T., Hughes, J., Jones, C.D., Joshi, M., Liddicoat, S., Martin, G., O'Connor, F., Rae, J., Senior, C., Sitch, S., Totterdell, I., Wiltshire, A., Woodward, S., 2011. Development and evaluation of an Earth-system model HadGEM2. Geosci. Model Dev. Discuss. 4, 997–1062.

Cooman, A., Schrevens, E., 2004. Sensitivity analyses of TOMGRO output variables to variations in climate conditions. Acta Hortic. 654, 317–324.

Costa, M., Heuvelink, E., 2007. Today's Worldwide Tomato Production. International Suppliers Guide 2007 – www.HortiWorld n.1.

Costa, J.M., Ortuño, M.F., Chaves, M.M., 2007. Deficit irrigation as a strategy to save water: physiology and potential application to horticulture. J. Integr. Plant Biol. 49, 1421–1434. https://doi.org/10.1111/j.1672-9072.2007.00556.x.

Danuso, F., 2002. Climak: a stochastic model for weather data generation. Ital. J. Agron.

6, 57–71.
Darand, M., Mansouri Daneshvar, M.R., 2015. Variation of agro-climatic indices in Kurdistan Province of Iran within 1962-2012. Model. Earth Syst. Environ. 1, 7. https://doi.org/10.1007/s40808-015-0010-9.
Déqué, M., Rowell, D.P., Lüthi, D., Giorgi, F., Christensen, J.H., Rockel, B., Jacob, D., Kjellström, E., de Castro, M., van den Hurk, B., 2007. An intercomparison ofregional climate simulations for Europe: assessing uncertainties in model projections. Clim. Change 81, 53–70.
Dimokas, G.C., Katsoulas, N., Kittas, C., Tchamitchian, M., 2012. Case studies of a modified biological simulator (TOMGRO) according to short cropping period. Acta Hortic. 952, 317–322.
Donatelli, M., et al., 2014. BioMA - Biophysical Model Application Framework. (verified March 6, 2019). https://en.wikipedia.org/wiki/BioMA.
Donatelli, M., Bellocchi, G., Carlini, L., Colauzzi, M., 2005. CLIMA: a component-based weather generator frameworks. In: Zerger, A., Argent, R.M. (Eds.), Eds.), MODSIM 2005 International Congress on Modeling and Simulation. Modeling and Simulation Society of Australia and New Zealand, Melbourne, Australia, pp. 627–633.
English, M., 1990. Deficit irrigation. I. Analytical framework. J. Irrig. Drain E. ASCE 116, 399–412.
Fereres, E., Soriano, M.A., 2007. Deficit irrigation for reducing agricultural water use. J. Exp. Bot. 58, 147–159. https://doi.org/10.1093/jxb/erl165.
Geerts, S., Raes, D., 2009. Deficit irrigation as an on-farm strategy to maximize crop water productivity in dry areas. Agric. Water Manag. 96, 1275–1284. https://doi.org/10.1016/j.agwat.2009.04.009.
Giannoccaro, G., Prosperi, M., Zanni, G., 2011. Economic effects of legislative framework changes in groundwater use rights for irrigation. Water 3, 906–922. https://doi.org/10.3390/W3030906.
Giorgi, F., Lionello, P., 2008. Climate change projections for the Mediterranean region. Glob. Planet. Change 63 (2–3), 90–104. https://doi.org/10.1016/j.gloplacha.2007.09.005.
Giuliani, M.M., Gatta, G., Nardella, E., Tarantino, E., 2016. Water saving strategies assessment on processing tomato cultivated in Mediterranean region. Ital. J. Agron. 11, 69–76. https://doi.org/10.4081/ija.2016.738.
Giuliani, M.M., Nardella, E., Gagliardi, A., Gatta, G., 2017. Deficit irrigation and partial root-zone drying techniques in processing tomato cultivated under Mediterranean conditions. Sustainability 9 (12), 2197. https://doi.org/10.3390/su9122197.
Giuliani, M.M., Gagliardi, A., Nardella, E., Carucci, F., Amodio, M.L., Gatta, G., 2019. The effect of strobilurin on ethylene production in flowers, yield and quality parameters of processing tomato grown under a moderate water stress condition in Mediterranean area. Sci. Hortic. 249, 155–161. https://doi.org/10.1016/j.scienta.2019.01.050.
IPCC, et al., 2013. Summary for policymakers. In: Stocker, T.F., Qin, D., Plattner, G.-K., Tignor, M., Allen, S.K., Boschung, J. (Eds.), Climate Change 2013: the Physical Science Basis. Contribution of Working Group I to the Fifth Assessment Report of the Intergovernmental Panel on Climate Change. Cambridge University Press, Cambridge, United Kingdom and New York, NY, USA, pp. 28.
IPCC, Qin, D., Manning, M., Chen, Z., Marquis, M., Averyt, K.B., Tignor, M., Miller, H.L., 2007. . IPCC summary for policymakers. Climate Change 2007: The Physical Science Basis. Contribution of Working Group I to the Fourth Assessment Report of the Intergovernmental Panel on Climate Change. Cambridge University Press, New York, NY, USA.
ISTAT, 2018. Rome (I): Italian National Institute of Statistics [updated YEAR, MONTH, DAY; Cited YEAR, MONTH, DAY]. Available from: http://. .
Jones, J.W., Dayan, E., Allen, L.H., Van Keulen, H., Challa, H., 1991. A dynamic tomato growth and yield model (TOMGRO). Trans. ASAE 34 (2), 0663–0672. https://doi.org/10.13031/2013.31715.
Jørgensen, S.E., Kamp-Nielsen, L., Christensen, T., Windolf-Nielsen, J., Westergaard, B., 1986. Validation of a prognosis based upon a eutrophication model. Ecol. Modell. 35, 165–182.
L'Abate, G., Fantappie, M., Priori, S., D'Avino, L., Barbetti, R., Lorenzetti, R., Costantini, E.A.C., 2019. Italian Derived Soil Profile's Database. 1.0.Consiglio Per La Ricerca in Agricoltura E l'analisi Dell'economia Agraria (CREA-AA). Online Database (Last access 23/05/2019). .
Lê, S., Josse, J., Husson, F., 2008. FactoMineR: an r package for multivariate analysis. J. Stat. Softw. 25 (1). https://doi.org/10.18637/jss.v025.i01.
Leolini, L., Fila, G., Costafreda-Aumedes, S., Ferrise, R., Bindi, M., 2018. Late spring frost impacts on future grapevine distribution in Europe. Field Crops Res. 222, 197–208. https://doi.org/10.1016/j.fcr.2017.11.018.
Louski, M., Linker, R., Teitel, M., 2013. Development of an object-oriented version of TOMGRO for a web-based decision support system. IFAC Agri. 121–126. https://doi.org/10.3182/20130828-2-SF-3019.00018. 2013.
Molden, D., 2003. A water-productivity framework for understanding and action. In: Kijne, J.W., Barker, R., Molden, D. (Eds.), Water Productivity in Agriculture: Limits and Opportunities for Improvement. International Water Management Institute, Colombo, Sri Lanka, pp. 1–18.
Montoya, F., Camargo, D.C., Dominguez, A., Ortega, J.F., Corcoles, J.J., 2018. Parametrization of Cropsyst model for the simulation of a potato crop in a Mediterranean environment. Agric. Water Manag. 203, 297–310. https://doi.org/10.1016/j.agwat.2018.03.029.
Nana, E., Corbari, C., Bocchiola, D., 2014. A model for crop yield and water footprint assessment: study of maize in the Po valley. Agric. Syst. 127, 139–149. https://doi.org/10.1016/j.agsy.2014.03.006.
Nash, J.E., Sutcliffe, J.V., 1970. River flow forecasting through conceptual models, part I-a discussion of principles. J. Hydrol. (Amst) 10, 282–290.
Nelder, J.A., Mead, R., 1965. A simplex method for function minimization comput. Comput. J. 7 (4), 308–3013. https://doi.org/10.1093/comjnl/7.4.308.
Nuruddin, M., Madramootoo, C.A., Dodds, G.T., 2003. Effects of water stress at different growth stages on greenhouse tomato yield and quality. Hort. Sci. 38, 1389–1393. https://doi.org/10.21273/HORTSCI.38.7.1389.
Onofri, A., Benincasa, P., Guiducci, M., Tei, F., 2009. Is CropSyst adequate for management-oriented simulation of growth and yield of processing tomato? J. Appl. Hortic. 1, 17–22.
Pathak, T.B., Stoddard, C.S., 2018. Climate change effects on the processing tomato growing season in California using growing degree day model. Model. Earth Syst. Environ. (MESE) 4, 765–775.
R Core Team, 2017. R: A Language and Environment for Statistical Computing. http://www.R-project.org/.
Raes, D., Steduto, P., Hsiao, T.C., Fereres, E., 2009. AQUACROP - the FAO crop model for predicting yield response to water: II. Main algorithms and software description. Agron. J. 101, 438–447. https://doi.org/10.2134/agronj2008.0139s.
Rinaldi, M., Garofalo, P., Rubino, P., Steduto, P., 2011. Processing tomatoes under different irrigation regimes in Southern Italy: agronomic and economic assessments in a simulation case study. Ital. J. Agrometeorol. 3, 39–56.
Ronco, P., Zennaro, F., Torresan, S., Critto, A., Santini, M., Trabucco, A., Zollo, A.L., Galluccio, G., Marcomini, A., 2017. A risk assessment framework for irrigated agriculture under climate change. Adv. Water Resour. 110, 562–578. https://doi.org/10.1016/j.advwatres.2017.08.003.
Rubino, P., Stelluti, M., Stellacci, A.M., Armenise, E., Ciccarese, A., Sellami, M.H., 2012. Yield response and optimal allocation of irrigation water under actual and simulated climate change scenarios in a southern Italy district. Ital. J. Agronom. 7 (18), 124–132. https://doi.org/10.4081/ija.2012.e18.
Saxton, K.E., Rawls, W.J., Romberger, J.S., Papendick, R.I., 1986. Estimating generalized soil-water characteristics from texture. Soil Sci. Soc. Am. J. 50, 1031–1036.
Schaeffer, D.L., 1980. A model evaluation methodology applicable to environmental assessment models. Ecol. Model. 8, 275–295. https://doi.org/10.2136/sssaj1986.03615995005000040039x.
Schmidt, G.A., Ruedy, R., Hansen, J.E., Aleinov, I., Bell, N., Bauer, M., Bauer, S., Cairns, B., Canuto, V., Cheng, Y., Del Genio, A., Faluvegi, G., Friend, A.D., Hall, T.M., Hu, Y., Kelley, M., Kiang, N.Y., Koch, D., Lacis, A.A., Lerner, J., Lo, K.K., Miller, R.L., Nazarenko, L., Oinas, V., Perlwitz, J., Rind, D., Romanou, A., Russell, G.L., Sato, M., Shindell, D.T., Stone, P.H., Sun, S., Tausnev, N., Thresher, D., Yao, M.S., 2006. Present day atmospheric simulations using giss model: comparison to in-situ, satellite and reanalysis data. J. Climate 19, 153–192. https://doi.org/10.1175/JCLI3612.1.
Scholberg, J.M.S., Boote, K.J., Jones, J.W., McNeal, B.L., 1987. Adaptation of the CROPGRO model to simulate the growth of field-grown tomato. Systems Approaches for Sustainable Agricultural Development: Applications of Systems Approaches at the Field Level: 133-151. Kluwer Academic Publ., Dordrecht, the Netherlands. https://doi.org/10.1007/978-94-017-0754-1_9.
Scotto, A., 2016. Between exploitation and protest: migrants and the agricultural gangmaster system in Southern Italy. REMHU, Rev. Interdiscip. Mobil. Hum. 24 (48). https://doi.org/10.1590/1980-85852503880004806. Brasília Sept./Dec.
Seidel, S.J., Palosuo, T., Thorburn, P., Wallach, D., 2018. Towards improved calibration of crop models – where are we now and where should we go? Eur. J. Agron. 94, 25–35. https://doi.org/10.1016/j.eja.2018.01.006.
Stella, T., Frasso, N., Negrini, G., Bregaglio, S., Cappelli, G., Acutis, M., Confalonieri, R., 2014. Model simplification and development via reuse, sensitivity analysis and composition: a case study in crop modeling. Environ. Model. Softw. 59, 44–58. https://doi.org/10.1016/j.envsoft.2014.05.007.
Stockle, C., Martin, A., Campbell, G.S., 1999. CropSyst, a cropping systems simulation model: Water/Nitrogen budgets and crop yield. Agric. Syst. 46, 335–359. https://doi.org/10.1016/0308-521X(94)90006-2.
Tarantino, E., Onofri, M., 1991. Determinazione dei coefficienti colturali mediante lisimetri. Bonifica 8, 119–136.
Tjiputra, J.F., Roelandt, C., Bentsen, M., Lawrence, D.M., Lorentzen, T., Schwinger, J., Seland, Ø., Heinze, C., 2013. Evaluation of the carbon cycle components in theNorwegian Earth System Model (NorESM). Geosci. Model. Dev. Discuss. 6, 301–325. https://doi.org/10.5194/gmdd-5-3035-2012.
USDA - Soil Survey Division Staff, 1993. Soil Survey Manual. Soil Conservation Service. U.S. Department of Agriculture Handbook 18 Chapter 3.
Vazquez-Cruz, M.A., Guzman-Cruz, R., Lopez-Cruz, I.L., Cornejo-Perez, O., Torres-Pacheco, I., Guevara-Gonzalez, R.G., 2014. Global sensitivity analysis by means of EFAST and Sobol' methods andcalibration of reduced state-variable TOMGRO model using genetic algorithms. Comput. Electron. Agric. 100, 1–12.
Ventrella, D., Charfeddine, M., Moriondo, M., Rinaldi, M., Bindi, M., 2012. Agronomic adaptation strategies under climate change for winter durum wheat and tomato in southern Italy: irrigation and nitrogen fertilization. Reg. Environ. Change 12, 407–419. https://doi.org/10.1007/s10113-011-0256-3.
Ventrella, D., Giglio, L., Garofalo, P., Dalla Marta, A., 2017. Regional assessment of green and blue water consumption for tomato cultivated in Southern Italy. J. Agric. Sci. https://doi.org/10.1017/S0021859617000831.
Vitale, D., Rana, G., Soldo, P., 2010. Trends and extremes analysis of daily weather data from a site in the Capitanata plain (Southern Italy). Ital. J. Agron. 5, 133–143. https://doi.org/10.4081/ija.2010.133.
Watanabe, S., Hajima, T., Sudo, K., Nagashima, T., Takemura, T., Okajima, H., Nozawa, T., Kawase, H., Abe, M., Yokohata, T., Ise, T., Sato, H., Kato, E., Takata, K., Emori, S., Kawamiya, M., 2011. MIROC-ESM 2010: model description and basicresults of CMIP5-20c3 m experiments. Geosci. Model. Dev. Discuss. 4, 845–872. https://doi.org/10.5194/gmd-4-845-2011.
Wickham, H., 2009. ggplot2: Elegant Graphics for Data Analysis. http://ggplot2.tidyverse.org/reference/.
Zhang, H., Oweis, T., 1999. Water-yield relations and optimal irrigation scheduling of wheat in the Mediterranean region. Agric. Water Manag. 38, 195–211. https://doi.org/10.1016/S0378-3774(98)00069-9.
Zubler, E.M., Fischer, A.M., Fröb, F., Liniger, M.A., 2016. Climate change signals of CMIP5 general circulation models over the Alps – impact of model selection. Int. J. Climatol. 36, 3088–3104. https://doi.org/10.1002/joc.4538.